

Self-similar Evolutionary Solutions for Accreting Magneto-fluid around a Compact Object with Finite Electrical Conductivity

F. Habibi^{1,*}, R. Pazhouhesh¹, and M. Shaghaghian²

¹ Department of Physics, Faculty of Sciences, University of Birjand , Birjand, Iran

² Department of Physics, Science and Research Branch, Islamic Azad University, Fars, Iran

The dates of receipt and acceptance should be inserted later

Key words accretion, accretion disk, magnetohydrodynamic.

In this paper, we investigate the time evolution an accreting magneto-fluid with finite conductivity. For the case of a thin disk, the fluid equations along with Maxwell equations are derived in a simplified, one-dimensional model that neglects the latitudinal dependence of the flow. The finite electrical conductivity is taken into account for the plasma through Ohm law; however, the shear viscous stress is neglected, as well as the self-gravity of the disk. In order to solve the integrated equations that govern the dynamical behaviour of the magneto-fluid, we have used a self-similar solution. We introduce two dimensionless variables, S_0 and ϵ_ρ , which show the magnitude of electrical conductivity and the density behaviour with time, respectively. The effect of each of these on the structure of the disk is studied. While the pressure is obtained simply by solving an ordinary differential equation, the density, the magnetic field, the radial velocity and the rotational velocity are presented analytically. The solutions show that the S_0 and ϵ_ρ parameters affect the radial thickness of the disk. Also, the radial velocity and gas pressure are more sensitive to electrical conductivity in the inner regions of disk. Moreover, the ϵ_ρ parameter has a more significant effect on physical quantities in small radii.

Copyright line will be provided by the publisher

1 Introduction

Accretion of gas onto compact objects can provide a powerful energy source for the production of high-energy radiation. When the gas infalls on a compact object, roughly 10% of the accreted rest mass energy could be converted into radiation. Thus, accretion is a process that can be considerably more efficient than many other common astrophysical mechanisms, such as nuclear fusion. Because the removal of the angular momentum process operates on slower timescales compared to the free-fall time, infalling gas with sufficiently high angular momentum can form a disk-like structure around a central compact object, which can be thin or thick depending on the geometrical shape. Theoretically, thin disks are well understood, based on a pioneering work by Shakura and Sunyaev (1973, hereafter SS73). However, for thick accretion disks, no fully developed model exists, and there remain many theoretical uncertainties about their structure and stability (Banerjee et al. 1995; Ghanbari & Abbassi 2004; Ghanbari et al. 2007).

It is generally believed that magnetic fields have a fundamentally important role in the physics of accretion disks. Magnetized accretion disks have been investigated by a number of authors in several different contexts: e. g., in relation to X-ray pulsars in closed binary systems (Ghosh & Lamb 1978; Aly 1980; Kaburaki 1986), to bipolar flows and jets from young stellar objects (Pudritz & Norman 1983; Kaburaki & Itoh 1987), and to quasars and active galactic nuclei (Blandford 1976; Blandford & Znajek 1977; Macdon-

ald & Thorn 1982). A mechanism for angular momentum transport is another key ingredient in the theory of accretion processes and many theoretical uncertainties still remain about its nature. A magnetic field can also contribute to the angular momentum transport. The angular momentum is transported by a global magnetic field which includes both poloidal and toroidal components of the ordered field (Kaburaki 2000). Additionally, a robust mechanism of the excitation of magnetohydrodynamical (MHD) turbulence was shown to operate in accretion disks as a result of the magnetorotational instability (Balbus & Hawley 1998; Begelman & Pringle 2007).

Because plasmas are electrically conducting gases, the influence of a magnetic field on the gas flow is quite complicated (Frank et al. 1992). In studying magnetized accretion disks from a theoretical point of view, there are two assumptions about the electrical conductivity of fluid. The first assumption is that the plasma disk has infinite conductivity, so that the magnetic fields of compact stars are completely confined within a certain distance and cannot penetrate the disk (Davidson & Osteriker 1973; Lamb et al. 1973; Aly 1980; Hayakawa 1985; Ogilvie 1997). The other assumption is that the electrical conductivity must be finite, which is taken into account through Ohm's law. The importance of finite conductivity was first pointed out by Ghosh and Lamb (1979), in the interaction of the accretion disks with the stellar magnetosphere. They showed that magnetic lines of force can penetrate the accretion disk owing to the presence of a finite resistivity. An analytical equilibrium solution, including the conductivity of the plasma for the case

* Corresponding author: e-mail: f.habibi@birjand.ac.ir

of a thin non-rotating magnetized star accreting matter from a disk, was obtained by Kaburaki (1986, 1987). He proposed a model for non-viscous, magnetized accretion disks, and showed that some features of this model are parallel to those of the standard model SS73 predicted for viscous, non-magnetic disks. Furthermore, he pointed out that the inclusion of finite conductivity is particularly essential for a disk in the absence of shear viscous, in order to liberate gravitational energy. Tripathy, Prasanna and Das(1990, hereafter TPD90) developed this analysis for thick disks and investigated their stability in the presence of a dipolar magnetic field due to a non-rotating central object. At the relativistic limit, Shaghaghian (2011) studied the dynamic of a stationary disk with finite conductivity around a rotating compact object with a dipole magnetic field. These studies have shown that the presence of a magnetic field and its associated finite conductivity can change the picture of accretion flows.

In this paper, we want to explore how the dynamic of a magneto-fluid depends on electrical conductivity. Thus, we pursue the approach adopted by TPD90 for an accreting magneto-fluid surrounding a non-rotating compact object. The essential difference in our calculations lies in the inclusion of the time-dependence of physical variables and the consideration of a thin geometrical configuration. So, we solve MHD equations for accreting gas that is self-similar over time. This paper is organized as follows. In section 2, we first define the general problem and derive the basic equations for magneto-fluid. Then, we use the self-similar method to solve the integrated equations that govern the dynamical behaviour of the accreting gas in section 3. Finally, we present a summary of the model in section 4.

2 General formulation

As mentioned above, we follow the general equations for a magneto-fluid in a manner similar to TPD90. In his approach, the Newtonian limit of the relativistic MHD equations are derived for an axisymmetric magneto-fluid in a spherical polar coordinate system, (r, θ, φ) , with the origin fixed on the non-rotating compact object. The accreting gas is highly ionized with finite electrical conductivity, and the poloidal model is adopted for the electromagnetic field, in which it has a poloidal component in the disk ($B_\varphi = E_\varphi = 0$). We also include time dependence for the matter distribution and electromagnetic fields. Thus, the Maxwell equations, which are used for MHD approximations, are obtained in the following form:

$$J_r = J_\theta = 0, \quad (1)$$

$$J_\varphi = -\frac{c}{4\pi r} \left[\frac{\partial}{\partial r} (rB_\theta) - \frac{\partial B_r}{\partial \theta} \right], \quad (2)$$

$$J_t = -\frac{1}{4\pi r^2} \left[\frac{\partial}{\partial r} (r^2 B_\theta V_\varphi) - \frac{r}{\sin \theta} \frac{\partial}{\partial \theta} (\sin \theta B_r V_\varphi) \right], \quad (3)$$

$$\frac{\partial}{\partial \theta} (r \sin \theta B_\theta) + \frac{\partial}{\partial r} (r^2 \sin \theta B_r) = 0, \quad (4)$$

$$\frac{\partial E_r}{\partial \theta} + \frac{\partial}{\partial r} (r E_\theta) = 0, \quad (5)$$

$$\frac{\partial}{\partial t} (r \sin \theta B_\theta) = 0, \quad (6)$$

$$\frac{\partial}{\partial t} (r^2 \sin \theta B_r) = 0. \quad (7)$$

Moreover, the electrical conductivity is taken into account through Ohm's law

$$J^i = \sigma F_{ik} u^k,$$

where J^i , F_{ik} and u^k are the current density, the electromagnetic field tensor and the four velocity vectors, respectively. The electrical conductivity of fluid, σ , is assumed to be constant throughout the disk. By neglecting toroidal fields, Ohm's law yields

$$E_r = \frac{B_\theta V_\varphi}{c}, \quad (8)$$

$$E_\theta = -\frac{B_r V_\varphi}{c}, \quad (9)$$

$$J_\varphi = -\frac{\sigma}{c} (B_\theta V_r - B_r V_\theta), \quad (10)$$

$$J_t = -\frac{\sigma}{c} (E_\theta V_\theta + E_r V_r) = \frac{J_\varphi V_\varphi}{c}. \quad (11)$$

The equations (2) and (10) are two different definitions for the azimuthal component of the current density. Their consistency yields

$$\frac{\partial}{\partial r} (r B_\theta) - \frac{\partial B_r}{\partial \theta} = \frac{4\pi \sigma r}{c^2} (B_\theta V_r - B_r V_\theta). \quad (12)$$

An admissible solution set for magnetic field that satisfies the equations (4), (6) and (7) is

$$B_r = -B_1 r^{k-1} \sin^{k-1} \theta \cos \theta, \quad (13)$$

$$B_\theta = B_1 r^{k-1} \sin^k \theta, \quad (14)$$

where k and B_1 are the constant values. From the above equations, we can see that the poloidal magnetic field does not depend explicitly on time. It has a similar configuration to the stationary disk (TPD90), which represents constant field lines parallel to the meridional plane. Substituting equations (13) and (14), the consistency relation (12) reduces to

$$V_r + V_\theta \cot \theta = \frac{(k-1)c^2}{4\pi \sigma r \sin^2 \theta}. \quad (15)$$

In the following, we consider a geometrically thin configuration, which means that the vertical thickness of the disk is sufficiently small, that we can assume $\theta = \pi/2$ and neglect terms associated with the θ -velocity ($V_\theta = 0$) and any θ dependence. The viscosity of the plasma has been ignored, since our purpose is analysing the role of electrical conductivity in an accreting gas. Also, the magnetic and electric stresses do not play a role in angular momentum transfer, due to the absence of the toroidal components of

the fields. The angular momentum transfer, therefore, occurs through the finite electrical resistivity of the plasma, $\eta = \frac{c^2}{4\pi\sigma}$, (Kaburaki 1987). For the sake of simplicity, the self-gravity of the disk is ignored in comparison with the gravitation of the central compact object. Consequently, the motion of plasma is governed by the continuity equation

$$\frac{\partial \rho}{\partial t} + \frac{1}{r^2} \frac{\partial}{\partial r}(r^2 \rho V_r) = 0, \quad (16)$$

and the momentum equations

$$\frac{\partial V_r}{\partial t} + V_r \frac{\partial V_r}{\partial r} + \frac{MG}{r^2} - \frac{V_\varphi^2}{r} + \frac{1}{\rho} \frac{\partial P}{\partial r} + \frac{B_\theta}{\rho} \frac{J_\varphi}{c} = 0, \quad (17)$$

$$\frac{\partial V_\varphi}{\partial t} + V_r \frac{\partial V_\varphi}{\partial r} + \frac{V_\varphi V_r}{r} = 0, \quad (18)$$

where P , ρ , V_r , V_φ denote the gas pressure, density, radial and azimuthal components of plasma velocity, respectively. Applying the thin disk approximation, the radial velocity is attained by the equation (15)

$$V_r = \frac{(k-1)c^2}{4\pi\sigma r}. \quad (19)$$

As a result, the radial velocity has the same form in steady (TPD90) and unsteady solutions. This is because the time derivative does not appear in the consistency relation. The equations of motion, (16), (17) and (18), are a set of non-linear partial differential equations, which cannot be solved analytically. Therefore, we search for solutions that describe the temporal change of physical quantities in such a way that the change of each quantity at any moment of time is similar to that of the others.

3 Self-similar solutions

3.1 Analysis

The equations of motion can be transformed into a set of ordinary differential equations by a temporal self-similar approach. The technique of self-similar analysis is familiar from its wide range of applications in the full set of equations of MHD in many research fields of astrophysics. A similarity solution, although constituting only a limited part of problem, is often useful in understanding the basic behaviour of the system. In a self-similar formulation, we introduce a similarity variable ξ as

$$\xi = \frac{r}{r_0(t)}, \quad (20)$$

wherein $r_0(t)$ follows a time-dependent power-law relation, as $r_0(t) = at^n$ and a, n are constants that are used to make ξ dimensionless. So, physical quantities (functions of r and t) are assumed as unknown time-dependent coefficients and functions of the dimensionless variable, ξ . We can determine the unknown time-dependent coefficients in a way that satisfies the basic equations. The resulting algebraic equations, which are only a function of the dimensionless variable ξ , can be solved analytically or semi-analytically. Therefore, we consider physical quantities in the following forms:

$$V_r(r, t) = v_0(t)V_r(\xi), \quad (21)$$

$$\rho(r, t) = \rho_0(t)\rho(\xi), \quad (22)$$

$$V_\varphi(r, t) = w_0(t)V_\varphi(\xi), \quad (23)$$

$$P(r, t) = p_0(t)P(\xi), \quad (24)$$

$$B_\theta(r, t) = b_0(t)B(\xi). \quad (25)$$

Also, we assume the electrical conductivity as

$$\sigma = S_0\sigma_0(t). \quad (26)$$

Here, we define S_0 as a conductivity dimensionless coefficient that is used to study the effect of electrical conductivity and as a free parameter. The equation (26) is necessary to create equations in a dimensionless form, since electrical conductivity has the dimension $time^{-1}$. Now, the equations (14) and (19) can be rewritten as

$$B_\theta(r, t) = \left(B_1 r_0(t)^{k-1} \right) \xi^{k-1}, \quad (27)$$

$$V_r(r, t) = \left(\frac{c^2}{4\pi\sigma_0(t)r_0(t)} \right) \frac{k-1}{S_0\xi}, \quad (28)$$

wherein

$$b_0(t) = B_1 r_0(t)^{k-1}, \quad B(\xi) = \xi^{k-1}, \quad (29)$$

$$v_0(t) = \frac{c^2}{4\pi\sigma_0(t)r_0(t)}, \quad V_r(\xi) = \frac{k-1}{S_0\xi}. \quad (30)$$

By substituting equations (20)-(26) into equations (16)-(18), the following relations are obtained

$$r_0(t) = (GM)^{1/3} t^{2/3}, \quad (31)$$

$$v_0(t) = (GM)^{1/3} t^{-1/3}, \quad (32)$$

$$p_0(t)/\rho_0(t) = (GM)^{2/3} t^{-2/3}, \quad (33)$$

$$w_0(t) = (GM)^{1/3} t^{-1/3}, \quad (34)$$

$$b_0(t)^2/\rho_0(t) = 4\pi(GM)^{2/3} t^{-2/3}, \quad (35)$$

$$\sigma_0(t) = \frac{c^2}{4\pi}(GM)^{-2/3} t^{-1/3}. \quad (36)$$

It should be mentioned that the current component J^φ in equation (17) has been inserted by equation (10). The above results imply that each physical quantity retains a similar spatial shape as the flow evolves, but the radius of the flow increases in proportion to $t^{2/3}$. In self-similar space, the time-dependent behaviour of the velocities is proportional to $t^{-1/3}$, namely, they decrease with time. Also, these relations show $p_0(t)$ and $b_0(t)$ are dependent on the behaviour of $\rho_0(t)$. Our results are in agreement with the previous findings for such time-dependent systems (Ogilvie 1999; Khesali & Faghei 2008, 2009). Moreover, self-similar solutions indicate that electrical conductivity is scaled with time as $t^{-1/3}$. This is a logical consequence of the dimensional consideration perspective.

For specifying the time dependence of $\rho_0(t)$, and then $p_0(t)$ and $b_0(t)$, we also assume a time-dependent power-law relation for density as

$$\rho_0(t) = R_0 t^{\epsilon_\rho}, \quad (37)$$

where R_0 is an arbitrary coefficient with the dimension of density \times time $^{-\epsilon_\rho}$. In order to evaluate the exponent ϵ_ρ , we employ the mass accretion rate \dot{M} :

$$\dot{M} = -4\pi r^2 \rho V_r. \quad (38)$$

Just like the equations (21)-(26) for the mass accretion rate, we can write:

$$\dot{M}(r, t) = \dot{M}_0(t) \dot{M}(\xi), \quad (39)$$

under transformations of equations (20), (21) and (22), equation (39) becomes

$$\dot{M}(r, t) = [r_0(t)^2 \rho_0(t) v_0(t)] [-4\pi \xi^2 \rho(\xi) V_r(\xi)], \quad (40)$$

which implies

$$\dot{M}_0(t) = r_0(t)^2 \rho_0(t) v_0(t), \quad (41)$$

$$\dot{M}(\xi) = -4\pi \xi^2 \rho(\xi) V_r(\xi). \quad (42)$$

By substituting equations (31), (32) and (37) into the equation (41), we obtain:

$$\dot{M}_0(t) = R_0(GM)t^{\epsilon_\rho+1}. \quad (43)$$

The above relation shows that when $\epsilon_\rho = -1$, $\dot{M}_0(t)$ is constant and decreases in $\epsilon_\rho < -1$. Accordingly, we can obtain a set of solutions for $\epsilon_\rho \leq -1$. Now, it is possible to derive the constant values of B_1 and k in equation (29), by using the equations (35) and (37). Thus, we obtain

$$B_1 = (4\pi R_0)^{\frac{1}{2}} (GM)^{\frac{1}{2}(2-k)}, \quad (44)$$

and

$$k = \frac{1}{2} \left(1 + \frac{3}{2} \epsilon_\rho \right). \quad (45)$$

Therefore, self-similar solutions show that the value of k is restricted by the ϵ_ρ parameter. This means that the spacial behavior of the magnetic field, in current time dependent solution, is determined by the ϵ_ρ parameter. However, as pointed out by TPD90, the magnetic field lines inside the disk do not depend on the value of k . Moreover, the magnetic moment of the disk, B_1 , is proportional to the matter distribution in the disk, while in the steady state, this parameter was obtained by boundary conditions and proportional to the surface magnetic field of the compact object. Also, by employing the equation (45), we find $V_r = -c^2/16\pi\sigma r$ for the maximum value of $k = -1/4$, whereas $V_r = -c^2/4\pi\sigma r$ for the maximum value of $k = 0$ in the steady solution. This indicates that although the radial dependence of infall velocity is same as the stationary disk, but its magnitude is changed when we consider the effects of continuously growing central mass.

3.2 Transformed basic equations

Substituting self-similar solutions (20)-(26) into the equations of motion, a set of ordinary differential equations is obtained as

$$\frac{d\rho(\xi)}{d\xi} \left[V_r(\xi) - \frac{2}{3}\xi \right] + \rho(\xi) \left[\frac{dV_r(\xi)}{d\xi} + 2\frac{V_r(\xi)}{\xi} + \epsilon_\rho \right] = 0, \quad (46)$$

$$-\frac{1}{3}V_r(\xi) + \left[V_r(\xi) - \frac{2}{3}\xi \right] \frac{dV_r(\xi)}{d\xi} - \frac{V_\varphi^2(\xi)}{\xi} + \frac{1}{\xi^2} + \frac{1}{\rho(\xi)} \frac{dP(\xi)}{d\xi} + S_0 \frac{B(\xi)^2}{\rho(\xi)} V_r(\xi) = 0, \quad (47)$$

$$\left[V_r(\xi) - \frac{2}{3}\xi \right] \frac{dV_\varphi(\xi)}{d\xi} + \left[\frac{V_r(\xi)}{\xi} - \frac{1}{3} \right] V_\varphi(\xi) = 0. \quad (48)$$

The equations (46) and (48) can be solved analytically by introducing $V_r(\xi)$ into them. Thus, the azimuthal velocity and the density distribution are

$$V_\varphi(\xi) = \frac{l}{\xi} \left[\xi^2 + \frac{3}{2} \frac{(1-k)}{S_0} \right]^{1/4}, \quad (49)$$

$$\rho(\xi) = \frac{1}{\xi} \left[\xi^2 + \frac{3}{2} \frac{(1-k)}{S_0} \right]^{\frac{1}{2}(1+\frac{3}{2}\epsilon_\rho)}. \quad (50)$$

Here, l is defined as the angular momentum parameter. It should be mentioned that the radial dependence of azimuthal velocity and density is different from steady solutions. Furthermore, in current solution, the azimuthal velocity is controlled by the electrical conductivity, as well as the radial velocity.

Finally, with the aid of the similarity functions $B(\xi)$, $V_r(\xi)$, $V_\varphi(\xi)$ and $\rho(\xi)$, a simple differential equation is obtained for the gas pressure:

$$\frac{dP(\xi)}{d\xi} = \frac{1}{\xi} \left[\xi^2 + \frac{3}{2} \frac{(1-k)}{S_0} \right]^{\frac{1}{2}(1+\frac{3}{2}\epsilon_\rho)} \left[\frac{1}{3} \frac{(1-k)}{S_0 \xi} - \frac{1}{\xi^2} + \frac{(1-k)^2}{S_0^2 \xi^3} + \frac{l^2}{\xi^3} \left(\xi^2 + \frac{3}{2} \frac{(1-k)}{S_0} \right)^{1/2} \right] - (1-k) \xi^{2k-3}. \quad (51)$$

This equation can be easily integrated by numerical methods. As a result, our solutions are sensitive to the S_0 and ϵ_ρ parameters. The S_0 parameter indicates the role of the electrical conductivity in the dynamics of the disk, and the ϵ_ρ parameter shows density changes with time. In fig. 1, we present our results for $\epsilon_\rho = -1$, the mass accretion rate of which is independent of time, and some values of S_0 . As this figure clearly shows, the radial inflow and azimuthal velocities become faster when the flow is inwards. The flow has differential rotations. An increase in S_0 slows down velocities and leads to an increase in density and a decrease in gas pressure. The gas pressure is a descending function of x , as well as of density distribution. Moreover, fig. 1c shows electrical conductivity's effect on the radial thickness of the disk; specifically, with increasing S_0 , the radial thickness of the disk increases. Also, as can be seen, the radial velocity and gas pressure are more sensitive to electrical conductivity in the inner regions of the disk. The behaviour of the radial velocity and density with respect to the electrical conductivity is qualitatively consistent with the results of TPD90.

Here, it is useful to compare the our results for a non-viscous disk with viscous disks. In viscous disks, the angular momentum is transported by the turbulent viscosity and the time-dependence of disk flow is controlled by the size

of the viscosity, α (Frank et al 2002). In our model for a non-viscous disk, as mentioned before, the transfer of angular momentum, which guarantees the successive accreting of matter, is carried by the electrical resistivity. The electrical resistivity has the same units as kinematic viscosity and we define the size of electrical resistivity as $\eta_0 = 1/S_0$ which can be considered corresponding to the viscous dimensionless parameter, α . We can also claim that the time-dependence of disk flow is controlled by the size of the electrical resistivity η_0 . Moreover, previous studies on the viscous disks (Akizuki & Fukue 2006; Khesali & Faghehi 2008) indicated that by increasing α parameter, the radial infall velocity increases, on the contrary, the density distribution decreases. Our self-similar solutions also show the η_0 parameter has similar effect on the radial velocity and density.

We plot fig.2 similarly to fig.1 for $S_0 = 0.6$ and some values of ϵ_ρ . This figure shows that both the radial and the azimuthal components of the velocity increases with increases in the absolute value of ϵ_ρ . This is contrary to the behaviour of the density and gas pressure, which reduce as the absolute of ϵ_ρ becomes larger. Moreover, the solutions show that the ϵ_ρ parameter is important at small radii. Panel (c) of fig. 2 indicates that the radial thickness of the disk decreases with increase of the absolute value of ϵ_ρ .

The effect of angular momentum parameter l on the distribution of pressure is demonstrated in fig.3(a). It shows that for higher values of l , the pressure increases. This result is qualitatively consistent with the results of TPD90. On the other hand, for an accreting magneto-fluid, the effective pressure has included gas pressure and magnetic pressure

$$\bar{P} = P + P_{mag} = P + \frac{B^2}{8\pi}. \quad (52)$$

We can show the importance of magnetic field pressure in comparison with the gas pressure by β parameter, which is defined as the ratio of the magnetic pressure to the gas pressure. By using the self-similar solutions (20)-(26), the β parameter takes the form

$$\beta(r, t) = \frac{B_\theta^2(r, t)/8\pi}{P(r, t)} = \frac{1}{2} \frac{B(\xi)^2}{P(\xi)}. \quad (53)$$

The above relation shows that the β parameter is independent of time. In other words, the fact that the time-dependent behaviour of the magnetic and gas pressures is similar limits the self-similarity solution. In contrast, physical quantities with the same physical dimension have similar behaviour (Khesali & Faghehi 2009). In fig.3(b), we plot the β parameter as a function of ξ for several values of S_0 . This figure indicates that the dominant pressure in the outer region of the disk is the magnetic pressure; this result is consistent with observed young stellar object disks (Aitken et al. 1993; Greave et al. 1997). The β parameter varies by S_0 ; that is, it increases by increasing the S_0 parameter, but this variation is important at larger radii.

By substituting equations (30) and (50) into equation (42), the function of $\dot{M}(\xi)$ is obtained as

$$\dot{M}(\xi) = \frac{4\pi(1-k)}{S_0} \left[\xi^2 + \frac{3(1-k)}{2S_0} \right]^k. \quad (54)$$

We plot $\dot{M}(\xi)$ as a function of ξ for some values of S_0 and ϵ_ρ in fig. 4. $\dot{M}(\xi)$ is very sensitive to the values of S_0 and ϵ_ρ . Therefore, these parameters are selected in smaller ranges. The figure displays the accretion rate is a function of position, and increases with decreasing radii, while in the steady state, it is a constant. As can be seen in fig. 4(a), when S_0 becomes smaller, the mass accretion rate increases. Such behaviour is similar to the behaviour of radial velocity. This is because radial velocity has more sensitivity to electrical conductivity than density (see equation 38). By contrast, the mass accretion rate decreases as the absolute of ϵ_ρ becomes larger.

4 Conclusions

The main aim of this manuscript was to examine the effect of electrical conductivity on the dynamic of accreting magneto-fluids. To this end, a self-similar solution has been derived for the equations of time-dependent accretion in a one-dimensional model. The plasma has been considered to be resistive with azimuthal and radial velocities. We have restricted ourselves to flow accretions in which self-gravitation and shear viscosity are negligible. In self-similar space, the electrical conductivity coefficient, σ , which is assumed to be constant throughout the disk, is scaled with time as $t^{-1/3}$ and a dimensionless free parameter, S_0 , is remained that demonstrates the size of electrical conductivity. In absent shear viscosity, both angular momentum transfer and energy dissipation in the flow is undertaken by the electrical resistivity whose size is specified by the $\eta_0 = 1/S_0$ parameter. The η_0 parameter can be considered corresponding to α parameter in standard model SS73.

The basic equations of dimensionless have been solved analytically. We obtained solutions parameterized by the temporal changes of density, ϵ_ρ , and the conductivity dimensionless coefficient, S_0 . The behaviour of physical quantities is determined for $\epsilon_\rho = -1$, where the mass accretion rate is independent of time, and also $\epsilon_\rho < -1$ which decreases with time. The solutions indicate that the S_0 parameter has a significant effect on the gas pressure and radial infall velocity in the inner regions of the disk. The radial thickness of the disk increases with greater S_0 parameter. Moreover, the solutions show the ϵ_ρ parameter is important in the inner regions of the disk. By increasing the absolute value of ϵ_ρ , the radial thickness of the disk decreases and the disk become compressed.

The previous studies of time dependent systems with infinite conductivity reveal the radial behaviour of physical quantities was different from the results achieved by those who considered stationary states (Khesali & Faghehi 2008, 2009). Our result, however, indicate that the radial dependence of the inflow velocity is similar to the solution of the stationary state which is reported by TPD90. This is a consequence of the presence of finite conductivity, which was taken in to account through Ohm law. We have also shown that the ratio of the magnetic pressure to the gas pressure is

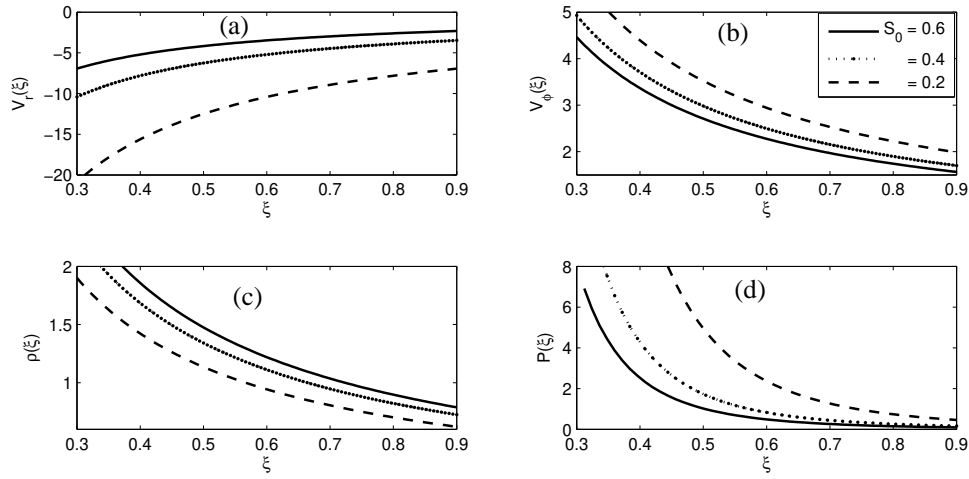


Fig. 1 The typical behavior of radial and azimuthal components of velocity, density and pressure as a function of dimensionless variable ξ for $\epsilon_\rho = -1$, $n = 1$ and some values of S_0 .

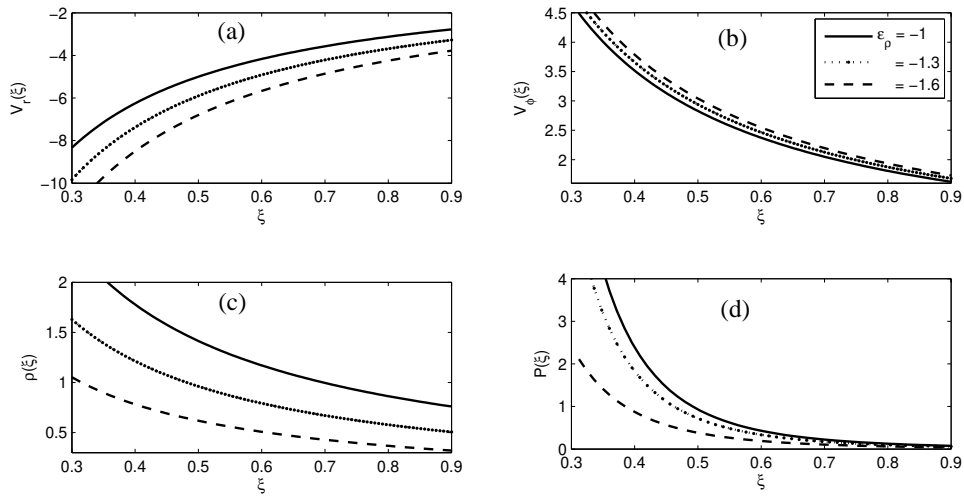


Fig. 2 Same as for fig.1 for $S_0 = 0.6$ and different values of ϵ_ρ

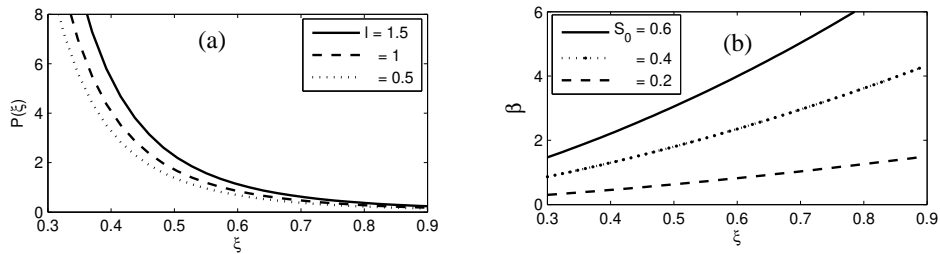


Fig. 3 Panel (a): the typical behavior of gas pressure for different values of n , constant values are $S_0 = 0.6$ and $\epsilon_\rho = -1$. Panel (b): the β parameter for $\epsilon_\rho = -1$ and different values of S_0 .

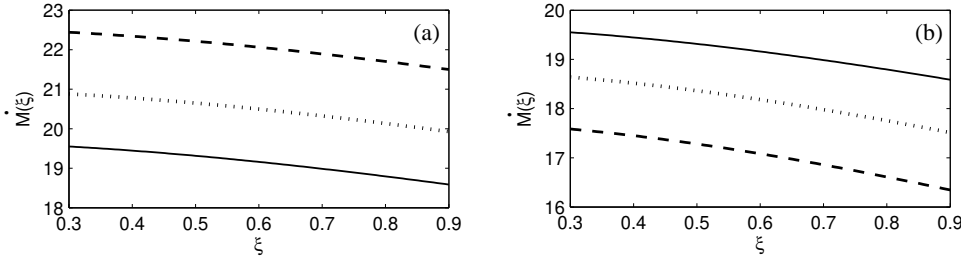


Fig. 4 Mass accretion rate as a function of dimensionless variable ξ . Panel (a): for $\epsilon_\rho = -1$, the solid lines represent $S_0 = 0.6$, the dotted lines represent $S_0 = 0.55$, and the dashed lines represent $S_0 = 0.5$. Panel (b): for $S_0 = 0.6$, the solid lines represent $\epsilon_\rho = -1$, the dotted lines represent $\epsilon_\rho = -1.1$, and the dashed lines represent $\epsilon_\rho = -1.2$.

a function of position, and increases when moving outward. This means that the magnetic field is more important at large radii. This ratio becomes larger by increasing the electrical conductivity of flow. Moreover, the solution shows that the mass accretion rate varies by radii and time and is very sensitive to values of S_0 and ϵ_ρ .

In our model, the latitudinal dependence of the physical quantities is ignored, but our understanding of the disk's properties could be improved by a discussion of two-dimensional models, in which one could explicitly treat both the radial and meridional structures of the accretion flow, and in which the thickness of the disk could be considered. In future studies, we will develop our model for thick disks.

- Khesali, A., Faghei, K.: 2008, MNRAS, 389, 1218
 Khesali, A., Faghei, K.: 2009, MNRAS, 398, 1361
 Lamb F.K., Pethick c.J., Pines D.: 1973, ApJ, 184, 271
 Macdonald, D.A., Thorn, K.S.: 1982, MNRAS, 198, 345
 Ogilvie, G.I.: 1997, MNRAS, 288, 63
 Ogilvie, G.I.: 1999, MNRAS, 306, 9
 Pudritz, R.E., Norman, C.A.: 1983, A&A, 274, 677
 Salpeter, E.E.: 1969, ApJ, 140, 796
 Shakura, N.I., Sunyaev, R.A.: 1973, ApJ, 24, 337
 Shadmehri, M.: 2004, MNRAS, 612, 1000
 Shaghaghian, M.: 2011, MNRAS, 415, 534
 Tripathy, S.C., Prasanna, A.R., Das A.C.: 1990, MNRAS, 246, 384(TPD90)

5 Acknowledgment

We are like to appreciate the referee for his/her thoughtful and constructive comments to improve this paper.

References

- Aitken, D. K., Wright, C. M., Smith, C. H., Roche, P. F.: 1993, MNRAS, 262, 456
 Akizuki C., Fukue J.: 2006, PASJ, 58, 469
 Aly, J., J.: 1980, A&A, 88, 192
 Balbus, S. A., Hawley, J.F.: 1998, Rev. Mod. Phys., 70, 1
 Banerjee, D., Bhatt, J.R., Das, A.C., Prasanna, A.R.: 1995, ApJ, 449, 789
 Begelman, M.C., Pringle, J.E.: 2007, MNRAS, 375, 1070
 Blandford, R.D.: 1976, MNRAS, 176, 465
 Blandford, R.D., Znajek, R.L.: 1977, MNRAS, 179, 433
 Davidson, K., Ostriker, J.P.: 1973, ApJ, 179, 585
 Frank, J., King, A., Raine, D.: 1992, Accretion Power in Astrophysics. Cambridge Univ. Press, Cambridge
 Ghanbari, J., Abbassi, S.: 2004, MNRAS, 350, 1437
 Ghanbari, J., Salehi, F., Abbassi, S.: 2007, MNRAS, 381, 159
 Ghosh, P., Lamb, F. K.: 1978, ApJ, 223, L83
 Ghosh, P., Lamb, F.K.: 1979, ApJ, 223, 259
 Greave, J.S., Holland, W.S., Ward-Thompson, D.: 1997, A&A, 480, 255
 Hayakawa, S.: 1985, A&AS, 92, 113
 Kaburaki, O.: 1986, MNRAS, 220, 321
 Kaburaki, O.: 1987, MNRAS, 229, 165
 Kaburaki, O.: 2000, ApJ, 531, 210
 Kaburaki, O., Itoh, M.: 1987, A&A, 172, 191